

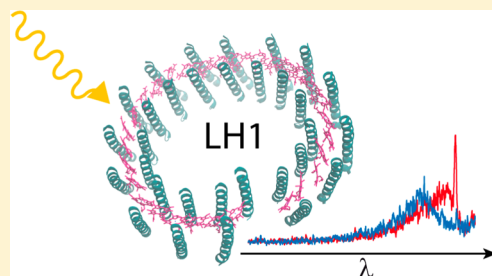
# Single-Molecule Spectroscopy on RC-LH1 Complexes of *Rhodopseudomonas acidophila* Strain 10050

Paul S. Böhm,<sup>†</sup> June Southall,<sup>‡</sup> Richard J. Cogdell,<sup>‡</sup> and Jürgen Köhler<sup>\*,†</sup>

<sup>†</sup>Experimental Physics IV and Bayreuth Institute for Macromolecular Research (BIMF), University of Bayreuth, 95440 Bayreuth, Germany

<sup>‡</sup>Institute of Molecular, Cell and Systems Biology, College of Medical Veterinary and Life Sciences, Biomedical Research Building, University of Glasgow, Glasgow G12 8QQ, Scotland, United Kingdom

**ABSTRACT:** We have revisited the RC-LH1 complex from *Rhodopseudomonas (Rps.) acidophila* for single-molecule spectroscopy. For the current study the pigment–protein complexes were stabilized in the detergent buffer solution using a relatively mild detergent (dodecyl- $\beta$ -D-maltoside (DDM) instead of lauryldimethylamine *N*-oxide (LDAO)). This leads to a significant reduction of the fraction of broken/dissociated RC-LH1 complexes with respect to previous studies and has allowed us to investigate a sufficiently large sample of individual RC-LH1 complexes. For most of the complexes the fluorescence–excitation spectra exhibit a narrow spectral feature at the red end of the spectrum. Analysis of the statistics of the spectral properties yields a close resemblance with the results obtained on RC-LH1 complexes from *Rps. palustris* for which a low-resolution X-ray structure is available. Based on this comparison we come to the conclusion that for both species the RC-LH1 complex can be described by the same structural model, that is, an overall elliptical assembly of pigments that features a gap.



## INTRODUCTION

Purple bacteria have evolved a wonderful modular principle for the light-harvesting (LH) apparatus that captures the solar radiation. These modules consist of pairs of hydrophobic, low molecular weight polypeptides, called  $\alpha$  and  $\beta$  (usually 50–60 amino acids long) that noncovalently bind a small number of bacteriochlorophyll (BChl) *a* and carotenoid (Car) molecules. These modules then oligomerize to produce the native circular or elliptical complexes.<sup>1–5</sup> Most purple bacteria have two main types of complexes, the core complex, RC-LH1, and the peripheral complex, LH2. In the NIR, LH2 has two strong absorption bands around 800 and 850 nm, respectively, whereas the RC-LH1 complex has a single strong absorption band around 880 nm. The LH1 complexes surround the reaction centers (RC) to form the so-called core complex. In contrast to LH2, where highly resolved X-ray structures are available,<sup>1–3</sup> the discussion in the literature about the structural properties of RC-LH1 complexes is much more controversial. The current view is that there are at least two distinct classes of RC-LH1 complexes. One class are monomeric; that is, they consist of one RC surrounded by one LH1 complex. An example of this class is the RC-LH1 complex from *Rps. palustris*.<sup>4</sup> The second class are dimeric; that is, they consist of two RC-LH1 units. An example of this class is the RC-LH1 complex from *Rhodobacter (Rb.) sphaeroides*.<sup>5</sup>

In the photosynthetic membrane the LH2 complexes are arranged in a two-dimensional network around the RC-LH1 complexes, and the light energy absorbed by LH2 is transferred via LH1 to the RC. In the RC the energy is used to drive a series of electron transfer reactions that result in the reduction

of ubiquinone (UQ).<sup>6</sup> After the secondary UQ<sub>B</sub> in the RC has been fully reduced to UQ<sub>B</sub>H<sub>2</sub>, the quinol must leave the RC in order to transfer its reducing equivalents to the Cytochrome *b*/*c*<sub>1</sub> complex, as part of a rather simple cyclic electron transport pathway.<sup>7</sup> There are two possibilities that may enable the passage of UQ<sub>B</sub>H<sub>2</sub> through the fence of  $\alpha\beta$  apoproteins of the surrounding LH1. Either the LH1 structure is inherently flexible enough to allow UQ<sub>B</sub>H<sub>2</sub> to diffuse through it,<sup>8</sup> or the LH1 ring is not complete; that is, there is a gap. The second option received substantial support when a protein called pufX was found in *Rb. sphaeroides*.<sup>9,10</sup> PufX appears to replace one of the  $\alpha\beta$ -dimers in the LH1 ring and thereby introduces a gap through which the UQ<sub>B</sub>H<sub>2</sub> could pass. The idea of an interruption in the LH1 structure was further substantiated when the first low resolution 4.8 Å X-ray crystal structure of the core complex from *Rps. palustris* was obtained.<sup>4</sup> In this complex the RC is enclosed by an overall elliptically shaped LH1 consisting of 15  $\alpha\beta$ -apoproteins each accommodating two BChl *a* molecules. Interestingly, adjacent to the RC UQ<sub>B</sub> binding site a gap was found instead of a 16th  $\alpha\beta$ -apoprotein pair. This gap is associated with a protein called W, which replaces an LH1  $\alpha\beta$ -dimer and which is believed to be an orthologue of pufX.

It is now well-established that the spatial arrangement of the pigments determines, to a large extent, the spectroscopic features of the complexes and that in these systems collective effects have to be considered to appropriately describe their

Received: January 16, 2013

Revised: February 26, 2013

Published: February 27, 2013

electronically excited states.<sup>11–28</sup> This leads to so-called Frenkel excitons, which arise from the interactions of the transition-dipole moments of the individual pigments, and which correspond to delocalized electronically excited states. The presence of a gap in the chromophore arrangement has severe consequences for the electronic structure of the complex and the photophysical parameters of the exciton states. First, degeneracies between the exciton states are lifted, and following common practice the exciton states are numbered  $k = 1, 2, \dots, N$ .<sup>29</sup> Second, significant oscillator strength is shifted to the lowest exciton state, that is,  $k = 1$ , in striking contrast to a closed-ring BChl *a* arrangement, as for example for LH2, where nearly all oscillator strength is accumulated in the next higher exciton states.<sup>14,24,30,31</sup> Since the fluorescence lifetime of the  $k = 1$  state is in the order of 600 ps<sup>32</sup> which is rather long with respect to the relaxation of the higher exciton states, that takes place on a 100 fs time scale,<sup>33,34</sup> this leads to the occurrence of a relatively narrow spectral feature at the red-edge of the absorption spectrum. Exploiting single-molecule spectroscopy those features could be made visible and not only confirmed the presence of the gap in LH1 from *Rps. palustris* but also gave rise to a refinement of details of the X-ray structure.<sup>22,23</sup>

To the best of our knowledge the first single-molecule experiments on RC-LH1 complexes were conducted by Ketelaars et al.<sup>25</sup> on those from the species *Rps. acidophila* for which up to date no structural information is available. This study was a follow up of the experiments on LH2 complexes from the same species.<sup>24,30,35</sup> Unfortunately, the resulting spectra revealed a large degree of spectral heterogeneity, and it was argued that in some of the complexes the LH1 rings were not fully intact or might even be decomposed. Meanwhile by means of simple room-temperature ensemble absorption experiments we found clear evidence for a partial dissociation of the RC-LH1 complexes if the complexes were stabilized in the detergent lauryldimethylamine *N*-oxide (LDAO), as it was used in the previous study.<sup>25</sup> Given the encouraging results obtained on RC-LH1 from *Rps. palustris*<sup>22,23</sup> we decided to revisit the species *Rps. acidophila* and use the milder detergent dodecyl- $\beta$ -D-maltoside (DDM) for stabilizing the complexes in the buffer solution.

A comparison of the room-temperature ensemble absorption spectra of RC-LH1 from *Rps. acidophila* obtained from complexes that were stabilized in the two detergents is shown in Figure 1. Both spectra feature the known BChl *a* absorption

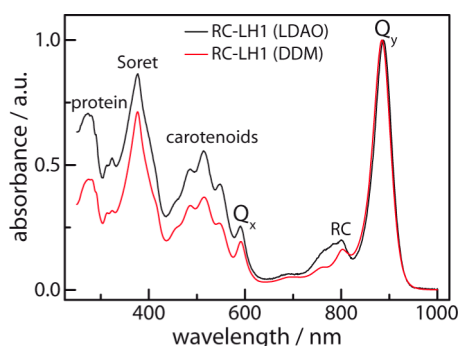


**Figure 1.** Room-temperature ensemble absorption spectra of RC-LH1 complexes from *Rps. acidophila* solubilized in LDAO (black line, data taken from ref 25) and DDM (red line). The assignments of the various bands are given in the figure. For better comparison the spectra have been normalized to the peak of the  $Q_y$  absorption bands.

bands ( $Q_y$ : 885/887.5 nm, DDM/LDAO;  $Q_x$ : 591.5/591 nm; Soret: 376.5/377 nm) as well as bands that can be attributed to the RC (803/799 nm), the carotenoids (515/514.5 nm, main peak), and the protein's aromatic residues (274/273 nm).<sup>36</sup> A commonly accepted measure for the purity of the sample is given by the ratio of the optical densities at 885 nm and at 280 nm,  $OD_{885}/OD_{280}$ , which amounts to 2.26 for the sample stabilized in DDM (Figure 1, red line) and 1.43 for the one in LDAO (Figure 1, black line), indicating the higher quality of the DDM sample. Another hint that the LDAO-stabilized RC-LH1 complexes might be partly broken is provided by the pronounced shoulder of the RC absorption band around 783 nm. This shoulder originates probably from free BChl *a* which absorbs around 770 nm<sup>36</sup> and is not observed for the DDM-stabilized sample.

In the present work we studied 61 individual DDM-stabilized RC-LH1 complexes from *Rps. acidophila* by fluorescence–excitation spectroscopy. For a large fraction of the complexes the observed spectra could be consistently explained with an exciton model based on the structural model for the species *Rps. palustris*.

## MATERIALS AND METHODS

**Sample Preparation.** *Rps. acidophila* strain 10050 was grown in Glasgow, and the RC-LH1 complexes were prepared as described previously<sup>37</sup> with the exception that once the RC-LH1 complexes were removed from the sucrose gradient centrifugation step, the detergent was exchanged from 0.1% LDAO into 0.02% DDM (Roth Chemie, Germany). This was carried out by binding the complexes to an anion exchange column, washing the bound complex with five column volumes of detergent buffer containing 0.02% DDM (20 mM Tris HCl, pH 8, 0.02% DDM), and then the bound complexes were eluted in 200 mM sodium chloride, 20 mM Tris HCl, pH 8.0, and 0.02% DDM. The RC-LH1 complexes were stabilized by this detergent exchange, and their concentration was adjusted to give an absorption of 100  $\text{cm}^{-1}$  ( $OD_{885}$ ) at 885 nm. This stock solution was transferred to Bayreuth where it was aliquoted, diluted to an  $OD_{885}$  of 10  $\text{cm}^{-1}$ , and stored in the dark at  $-80^\circ\text{C}$  until use. For single-molecule spectroscopy the RC-LH1 complexes were further diluted in several steps to about  $10^{-11}$  M in a similar detergent buffer solution as mentioned above. During the last dilution step 1% (w/w) polyvinyl alcohol (PVA;  $M_w = 124\,000$ – $186\,000$  g/mol; Sigma-Aldrich, Milwaukee, WIS, USA) was added to the sample. These preparations were done at room temperature in the dark to minimize any photodamage of the sample. Subsequently, a drop of this solution was spin-coated in an inert nitrogen atmosphere onto a quartz substrate for 15 s at 500 rpm and 60 s at 2000 rpm (model P6700; Specialty Coating System, Indianapolis, IN, USA). This resulted in an amorphous polymer film with a thickness of about 50–70 nm. Then the sample was immediately mounted in a helium-bath cryostat and cooled down to 1.2 K.

**Optical Setup.** Fluorescence–excitation spectroscopy was conducted in a home-built microscope that can be operated either in wide-field or confocal mode.<sup>19</sup> For excitation of the samples a continuous-wave tunable titanium–sapphire laser (3900S, Spectra Physics, Mountain View, CA, USA) was pumped by a frequency-doubled continuous-wave neodymium:yttrium–vanadate (Nd:YVO<sub>4</sub>) laser (Millennia Vs, Spectra Physics). Precise changes of the wavelength of the titanium:sapphire laser were accomplished by rotating the intracavity

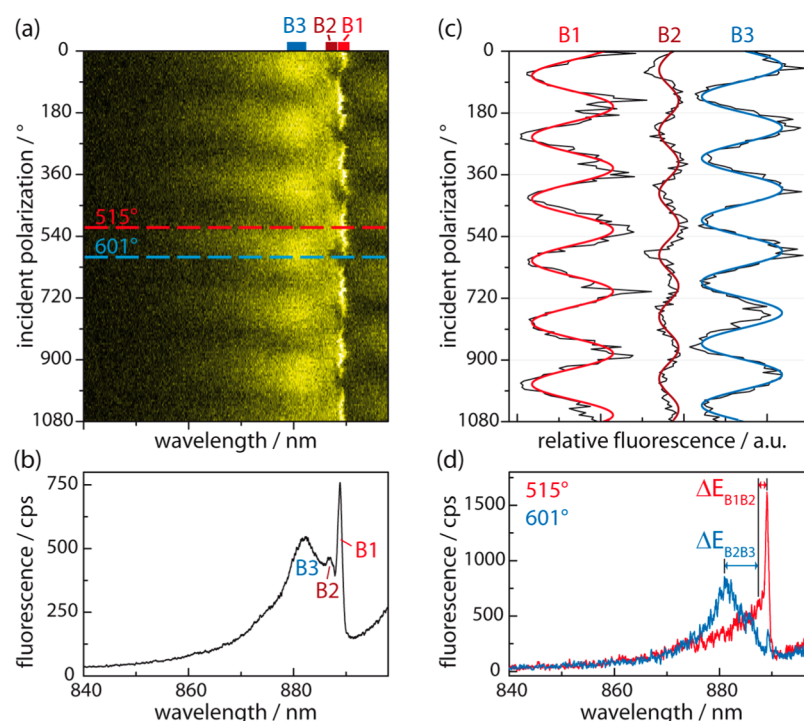


**Figure 2.** Fluorescence–excitation spectrum from an individual RC-LH1 complex from *Rps. acidophila* as a function of the polarization of the excitation light. (a) Stack of 174 consecutively recorded individual spectra. Between two successive spectra the polarization of the incident radiation has been rotated by  $6.2^\circ$ . The horizontal axis corresponds to the excitation wavelength, the vertical axis to the scan number, or equivalently to the polarization angle, and the intensity is given by the color code. The excitation intensity was  $300 \text{ W/cm}^2$ . (b) Spectrum that corresponds to the average of the 174 consecutively recorded spectra. (c) Integrated fluorescence intensity of the three spectral intervals B1–B3 that are indicated at the top of the panel in part (a), as a function of the polarization of the incident radiation (black lines). The colored lines correspond to  $\cos^2$ -type functions that have been fitted to the data. (d) Average of three adjacent spectra that have been recorded for polarizations where the distinct spectral features B1 (red) and B3 (blue) are most pronounced. The positions of the spectra within the stack displayed in part a are indicated by the dashed lines.

birefringent filter with a motorized micrometer screw. The accuracy as well as the reproducibility of the laser frequency were verified with a wavemeter and were about  $1 \text{ cm}^{-1}$ .

Initially a  $(40 \times 40) \mu\text{m}^2$  wide-field fluorescence image from the sample was recorded by exciting the sample with light at  $885 \text{ nm}$  that had passed a band-pass filter (BP 875/50, AHF Analysetechnik, Tübingen, Germany). The fluorescence emitted from the sample was collected by a microscope objective (Microthek, Hamburg, Germany,  $\text{NA} = 0.85$ ) that was mounted in the cryostat, and the signal was registered with a back-illuminated CCD camera (512 SB, Princeton Instruments, Trenton, NJ, USA) after passing a set of band-pass filters (BP 925/40, AHF Analysetechnik) that blocked backscattered laser light.

Next, the microscope was switched to the confocal mode. Using a pair of telecentric lenses and a mirror mounted on a gimbal mount the confocal volume was moved to coincide with a spatially well-isolated RC-LH1 complex that was selected from the wide-field image. Fluorescence–excitation spectra from single RC-LH1 complexes were recorded by scanning the laser repetitively between  $836$  and  $899 \text{ nm}$  and detecting the emitted fluorescence with a single-photon counting avalanche photodiode (APD) (SPCM-AQR-16, PerkinElmer, Vaudreuil, Canada) after passing a set of four band-pass filters (BP 925/40, AHF Analysetechnik). The recorded traces were stored separately in computer memory. The scan speed was  $2 \text{ nm/s}$  ( $\approx 26 \text{ cm}^{-1}/\text{s}$ ), and the acquisition time was  $10 \text{ ms}$ , which yields a nominal resolution of about  $0.26 \text{ cm}^{-1}$ , ensuring that the spectral resolution is limited by the spectral bandwidth of

the laser of  $1 \text{ cm}^{-1}$ . To examine the polarization dependence of the spectra, a  $\lambda/2$ -plate was turned by  $3.1^\circ$  between two successive scans. This changes the angle of the polarization of the excitation light by twice this value. All spectra were corrected for the variation of the incident laser intensity as a function of the excitation wavelength. Typically the excitation intensity was about  $250 \text{ W/cm}^2$ , and all experiments were conducted at  $1.2 \text{ K}$ .

## RESULTS AND DISCUSSION

The fluorescence–excitation spectra from individual RC-LH1 complexes were recorded as a function of the polarization of the excitation light. The laser was scanned repetitively between  $836$  and  $899 \text{ nm}$ , and between two successive scans the polarization of the incident radiation was rotated by  $6.2^\circ$ .

An example for this protocol is shown in Figure 2. The resulting spectra are shown in Figure 2a in a two-dimensional representation, where 174 individual scans have been stacked on top of each other. The horizontal axis corresponds to wavelength, the vertical axis to the polarization of the excitation, and the detected fluorescence intensity is given by the color code. Averaging all individual spectra yields the sum spectrum displayed in Figure 2b. It shows three spectral features denoted as B1–B3 that peak at  $889 \text{ nm}$ ,  $887 \text{ nm}$ , and  $882 \text{ nm}$ , respectively. Subsequently, in each individual spectrum the intensity of the bands B1–B3 was integrated over a small wavelength interval as indicated by the bars on top of Figure 2a, and the result is displayed in Figure 2c as a function of the



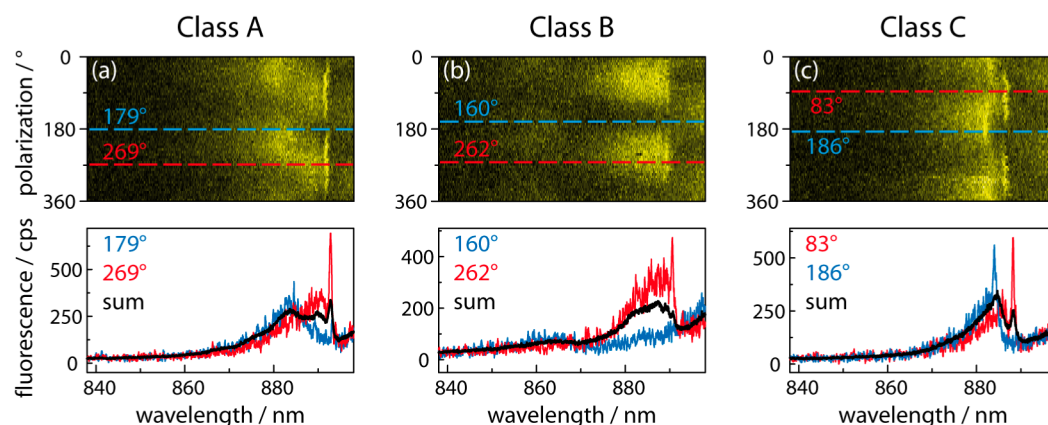


**Figure 3.** Classes of fluorescence–excitation spectra obtained from different RC-LH1 complexes from *Rps. acidophila*. The upper panels a, b, and c show stacks of consecutively recorded fluorescence–excitation spectra that have been restricted to 58 spectra each for brevity. Between two individual fluorescence–excitation spectra the polarization of the incident radiation has been rotated by  $6.2^\circ$ , and the fluorescence intensity is indicated by the color code. The spectra displayed at the bottom of each panel correspond either to the sum of the full stack of spectra (black lines), or to the average over three adjacent individual spectra (blue/red) that have been recorded for a distinct polarization of the excitation (indicated by the dashed colored lines in the top panels). In each case the vertical axis of the lower panels is valid for all three traces. The excitation intensity was typically about  $250 \text{ W/cm}^2$ .

polarization (black lines). For all three bands the intensity shows a modulation that is consistent with a  $\cos^2$ -dependence (colored lines). From this procedure we obtain the mutual angle between the transition-dipole moments of the bands that amount to  $\Delta\alpha_{B1B2} = 17^\circ$  for B1 and B2, and  $\Delta\alpha_{B2B3} = 79^\circ$  for B2 and B3, respectively. Finally, Figure 2d displays two spectra that have been recorded for those polarizations where the bands B1 (red) and B3 (blue) feature the maximum intensity. To improve the signal-to-noise ratio, each spectrum in Figure 2d corresponds to the average of three consecutive individual laser scans. This approach provides the energetic separations between the spectral bands which are  $\Delta E_{B1B2} = 26 \text{ cm}^{-1}$  and  $\Delta E_{B2B3} = 60 \text{ cm}^{-1}$  for this example.

Generally, the excitation spectra featured a few broad bands with linewidths (fwhm) varying between  $100 \text{ cm}^{-1}$  and  $290 \text{ cm}^{-1}$ . Most of the complexes (49/61 corresponding to 80%) featured in addition at least one narrow absorption line. The widths of these lines varied between  $3 \text{ cm}^{-1}$  and  $12 \text{ cm}^{-1}$  for the complexes. According to their spectral profiles, the complexes could be grouped into three categories, referred to as A–C, hereafter. A typical example for each category is shown in Figure 3. For each category the top panel displays a stack of 58 consecutively recorded fluorescence–excitation spectra as a function of the polarization of the excitation. Below these patterns the sum spectrum (black line) is shown together with example spectra (colored lines), each corresponding to the average of three consecutive scans, that feature the characteristic spectral details of each category.

The complexes attributed to category A (50 of 61 complexes) featured two broad bands with distinctly different orientation of their transition-dipole moments; see Figure 3a. For 38 of these complexes we observed a narrow spectral feature at the low-energy side of the fluorescence–excitation spectra. For the other 12 complexes the spectrum overlaps with the detection window, possibly masking a narrow line at the red end of the spectrum. The complexes assigned to class B (4/61) feature a single, linear polarization of the whole spectrum, Figure 3b. For all four complexes the registered fluorescence–excitation spectra exhibit a broad band with a narrow line at the low-energy wing. Finally in category C (7/61) the complexes

featured either two narrow lines, each one on the red wing of a broad absorption band, or a broad band on the red side of a narrow line extending into the detection window which presumably masks a second narrow line, Figure 3c.

Given that the majority of the RC-LH1 complexes featured category A spectra we will focus on these type of spectra in the following. In Figure 4 the distributions of the separations of the spectral bands and the mutual orientations of the associated transition-dipole moments are summarized.

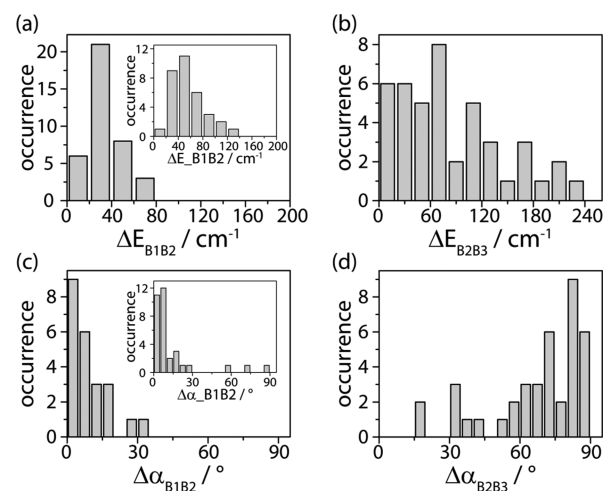


**Figure 4.** Distributions of the energetic separations  $\Delta E$  observed between (a) B1 and B2 and (b) B2 and B3 and of the mutual angles  $\Delta\alpha$  between the transition-dipole moments that are associated with (c) B1 and B2 and (d) B2 and B3. The insets in a and c display the corresponding data for RC-LH1 from *Rps. palustris* and have been taken from ref 23.

The histograms in Figure 4 differ from each other in the number of entries, which reflects the fact that for some complexes the spectra were red-shifted to an extent that they overlapped with the detection window, preventing the observation of all spectral bands. In particular, for 23 complexes only was the narrow feature at the red end of the spectrum observable and spectrally sufficiently stable to allow a reliable fit

of the relative phase angle. Only these complexes were considered for the histogram shown in Figure 4c. Similarly, for 11 of the category A complexes the energetic separation between B2 and B3 was so small that a reliable determination of the relative phase angle of the associated transition-dipole moments was impossible, which reduced the number of entries in the histogram shown in Figure 4d from 50 to 39. For the energy difference between the bands B1 and B2 (B2 and B3) we find a variation between  $2\text{ cm}^{-1}$  and  $68\text{ cm}^{-1}$  ( $3\text{ cm}^{-1}$  and  $236\text{ cm}^{-1}$ ), with a mean value of  $33\text{ cm}^{-1}$  ( $85\text{ cm}^{-1}$ ), Figure 4a,b. To restrict the scale for the relative orientations of the transition-dipole moments to values between  $0^\circ$  and  $90^\circ$  the phase differences were calculated as  $\Delta\alpha_{B_iB_j} = |\alpha_{B_i} - \alpha_{B_j}|$  if the result was less than  $90^\circ$  or as  $\Delta\alpha_{B_iB_j} = 180^\circ - |\alpha_{B_i} - \alpha_{B_j}|$  otherwise. Accordingly, the distribution of the relative orientations of the transition-dipole moments that are associated with B1 and B2 displays a maximum at about  $0^\circ$  and a steep decrease for larger angles, Figure 4c. For the bands B2 and B3 the respective distribution for the mutual orientation of the transition-dipole moments increases from  $15^\circ$  to a maximum at about  $90^\circ$ , Figure 4d.

The insets in Figure 4a,c show the distributions for the energy splitting,  $\Delta E_{B_1B_2}$ , and the mutual angle between the corresponding transition-dipole moments,  $\Delta\alpha_{B_1B_2}$ , for the bands B1 and B2 of RC-LH1 from *Rps. palustris* and were taken from ref 23. Given the similarity of these distributions with the data from *Rps. acidophila*, it can be concluded that the *palustris* model described in ref 23 also grasps the essential features of the RC-LH1 structure from *Rps. acidophila*. In ref 23, the experimental data were compared with results from numerical simulations based on a simple model Hamiltonian using the Heitler–London approximation, and it was found that the RC-LH1 complexes from *Rps. palustris* can be adequately modeled by 15 BChl *a* dimers that are distributed equidistantly around an ellipse that features a gap adjacent to the RC UQ<sub>B</sub> binding site. In analogy with the *palustris* study we assign the observed spectral bands B1, B2, and B3 to the exciton states  $k = 1, 2, 3$ , respectively, where B3 may have additional contributions from exciton states  $k > 3$  depending on the specific realization of diagonal disorder. A more profound statement about further structural details of the LH1 aggregates of the bacterial species *Rps. palustris* and *Rps. acidophila* or differences between them requires a more sophisticated theoretical approach than Heitler–London and a dipole–dipole approximation, for obtaining better information about the site energies of the individual BChl *a* molecules and the intermolecular interaction strengths, respectively.<sup>38</sup> In particular those BChl *a* molecules adjacent to the gap are expected to have distinctly different site energies with respect to the other BChl *a* molecules in the assembly due to their different protein environment.

Unfortunately the distributions for the energy separations  $\Delta E_{B_2B_3}$  and the mutual angles  $\Delta\alpha_{B_2B_3}$  of the associated transition-dipole moments for the bands B2 and B3 are not available for the *Rps. palustris* study, and so we have compared our results with those from the study of Ketelaars et al.<sup>25</sup> on RC-LH1 from *Rps. acidophila* where the focus was predominantly on these two broad bands. In that study four types of spectra (I–IV) were distinguished that correspond to the classes A–C that are used here as given in Table 1.

The analysis of the spectra presented in Ketelaars et al.<sup>25</sup> was based on work performed on LH2 complexes from the same

**Table 1. Influence of the Type of Detergent on the Occurrence of RC-LH1 Complexes from *Rps. acidophila* with Distinct Spectral Features**

class	detergent DDM (present work)		detergent LDAO <sup>25</sup>	
	relative fraction (number of complexes)		type	relative fraction (number of complexes)
A	82% (50)		I + II	46% (7 + 4)
B	6.5% (4)		III	16.5% (4)
C	11.5% (7)		IV	37.5% (9)

species.<sup>24,35</sup> In LH2 the B850 BChl *a* molecules form a closed ring, that, in first approximation, gives rise to a (circular) exciton structure with pairwise degenerate exciton states  $k^{\text{circ}} = \pm 1, \pm 2, \dots$  and two nondegenerate states  $k^{\text{circ}} = 0, 9$ . Appreciable oscillator strength is found only for the states  $k^{\text{circ}} = \pm 1$  which feature mutually orthogonal transition-dipole moments. Ketelaars et al. interpreted the two broad spectral features (here denoted as B2 and B3) as the  $k^{\text{circ}} = \pm 1$  exciton states of a closed ring structure in analogy with the LH2 case. The more frequent observation of a narrow spectral feature for RC-LH1 with respect to LH2 (interpreted to stem from  $k^{\text{circ}} = 0$ ) was ascribed to the fact that in RC-LH1 the structural heterogeneity leads to a more pronounced mixing of the exciton levels and subsequent redistribution of oscillator strength due to the higher density of exciton states in LH1 with respect to LH2. As a consequence of this, they classified spectra that featured both a narrow spectral line at the red end of the spectrum, as well as a mutual angle between the transition-dipole moments of the two following, red-shifted, broad bands around  $90^\circ$  (here denoted as  $\Delta\alpha_{B_2B_3}$ ) as type I, and spectra where these bands featured a phase difference between  $30^\circ$  and  $65^\circ$  as type II. However, single-molecule work on RC-LH1 from *Rps. palustris* and on mutants from *Rb. sphaeroides*, that is, an open ring and a closed ring structure, has revealed that the frequent occurrence of the narrow spectral feature at the red end of the spectrum is a strong indication for a pigment arrangement with a gap.<sup>22,23</sup> For the current study, therefore the distinction between type I and type II spectra has been omitted, and all spectra that featured two broad bands with distinctly different oriented transition-dipole moments were classified as class A. Merging the data for type I and type II spectra in ref 25 yields for the energy separation (mean  $\pm$  sdev)  $\Delta E_{B_2B_3} = (122 \pm 64)\text{ cm}^{-1}$  and for the mutual angle of the transition dipole moments  $\Delta\alpha_{B_2B_3} = (71 \pm 22)^\circ$  which can be compared with  $(85 \pm 60)\text{ cm}^{-1}$  and  $(67 \pm 20)^\circ$  found here. Within their error margins the energetic separations roughly agree with each other, and the limited statistics of the previous study, where only 11 complexes contributed to the type I and type II spectra, should be kept in mind. The mutual orientations of the transition-dipole moments between the bands B2 and B3 is consistent with the previous work and, as stated already in ref 25, the observed strong deviation from a mean around  $90^\circ$  (in contrast to what has been observed for  $k^{\text{circ}} = \pm 1$  for LH2 complexes from *Rps. acidophila*<sup>39,40</sup>) might reflect an orientational distribution of the RC-LH1 complexes with respect to the plane of the polymer film. For the LH2 complexes it is believed that the electrostatic interaction between the complexes and the substrate in combination with the laminar flow induced by the spin-coating process entails a planar alignment of the LH2 complexes on the substrate.<sup>25</sup> In RC-LH1 however the RC protrudes by about  $20\text{ \AA}$  from the N-terminus side of the LH1 ring<sup>41</sup> which might tilt the plane of

the LH1 ring with respect to the substrate. As a result only the projections of the exciton transition-dipole moments on the plane perpendicular to the optical axis can be observed.

Finally we want to briefly address complexes that featured spectra classified as B and C. Class B spectra would be consistent with RC-LH1 complexes that are tilted so far that they are oriented with the plane of the BChl *a* ring perpendicular to the substrate, whereas class C spectra could originate from two molecular aggregates in close proximity to each other. A probable explanation for this is that these spectra stem from broken RC-LH1 complexes that were in the process of dissociation prior to cooling them down to cryogenic temperatures. For RC-LH1 complexes sustained in LDAO, tracers for such dissociation processes were already observed in the room-temperature absorption spectrum of the stock solution, see Figure 1.

If our interpretation of the spectral properties for the different classes is correct the fraction of broken/dissociated RC-LH1 complexes (here class C, type IV in ref 25) from *Rps. acidophila* can be significantly reduced by using DDM instead of LDAO as detergent, namely from 37.5% to 11.5%. The improved quality of the stock solution allowed us to perform polarization-resolved fluorescence–excitation spectroscopy, and to determine the distributions of the spectral properties with a reasonable statistics. We find that the spectra from RC-LH1 from *Rps. acidophila* resemble in shape and statistical properties those obtained on RC-LH1 from *Rps. palustris* in an earlier study<sup>22,23</sup> and come to the conclusion that both structures can be described by the same structural model.

## AUTHOR INFORMATION

### Corresponding Author

\*Telephone: +49 921 55 4000. Fax: +49 921 55 4002. E-mail: juergen.koehler@uni-bayreuth.de.

### Notes

The authors declare no competing financial interest.

## ACKNOWLEDGMENTS

P.S.B. and J.K. gratefully acknowledge financial support from the Deutsche Forschungsgemeinschaft (KO 1359/16-1, GRK1640) and the state of Bavaria within the initiatives “Elite Network of Bavaria” (Lead Structures of Cell Function) and “Solar Technologies go Hybrid”. R.J.C. thanks the BBSRC for financial support.

## ABBREVIATIONS

RC, reaction center; LH1, light harvesting 1 (complex); LH2, light harvesting 2 (complex); BChl, bacteriochlorophyll; DDM, dodecyl- $\beta$ -D-maltoside; LDAO, lauryldimethylamine *N*-oxide; sdev, standard deviation

## REFERENCES

- (1) McDermott, G.; Prince, S. M.; Freer, A. A.; Hawthornthwaite-Lawless, A. M.; Papiz, M. Z.; Cogdell, R. J.; Isaacs, N. W. Crystal Structure of an Integral Membrane Light-Harvesting Complex from Photosynthetic Bacteria. *Nature* **1995**, *374*, 517–521.
- (2) McLuskey, K.; Prince, S. M.; Cogdell, R. J.; Isaacs, N. W. The Crystallographic Structure of the B800–820 LH3 Light-Harvesting Complex from the Purple Bacteria *Rhodospseudomonas acidophila* Strain 7050. *Biochemistry* **2001**, *40*, 8783–8789.
- (3) Koepke, J.; Hu, X.; Muenke, C.; Schulten, K.; Michel, H. The Crystal Structure of the Light-Harvesting Complex II (B800–B850) from *Rhodospirillum rubrum*. *Structure* **1996**, *4*, 581–597.
- (4) Roszak, A. W.; Howard, T. D.; Southall, J.; Gardiner, A. T.; Law, C. J.; Isaacs, N. W.; Cogdell, R. J. Crystal Structure of the RC-LH1 Core Complex from *Rhodospseudomonas palustris*. *Science* **2003**, *302*, 1969–1971.
- (5) Qian, P.; Hunter, N. C.; Bullough, P. A. The 8.5 Å Projection Structure of the Core RC-LH1-PufX Dimer of *Rhodobacter sphaeroides*. *J. Mol. Biol.* **2005**, *349*, 948–960.
- (6) Feher, G.; Allen, J. P.; Okamura, M. Y.; Rees, D. C. Structure and Function of Bacterial Photosynthetic Reaction Centres. *Nature* **1989**, *339*, 111–116.
- (7) Petty, K.; Jackson, J. B.; Dutton, P. L. Factors Controlling the Binding of Two Protons per Electron Transferred Through the Ubiquinone and Cytochrome *b*/*c*<sub>2</sub> Segment of *Rhodospseudomonas sphaeroides* Chromatophores. *Biochim. Biophys. Acta* **1979**, *546*, 17–42.
- (8) Aird, A.; Wrachtrup, J.; Schulten, K.; Tietz, C. Possible Pathway for Ubiquinone Shuttling in *Rhodospirillum rubrum* Revealed by Molecular Dynamics Simulation. *Biophys. J.* **2007**, *92*, 23–33.
- (9) Barz, W. P.; Francia, F.; Venturoli, G. B.; Melandri, A.; Vermeglio, A.; Oesterhelt, D. Role of the PufX Protein in Photosynthetic Growth of *Rhodobacter sphaeroides*. 1. PufX is Required for Efficient Light-Driven Electron Transfer and Photophosphorylation Under Anaerobic Conditions. *Biochemistry* **1995**, *34*, 15235–15247.
- (10) Barz, W. P.; Vermeglio, A.; Francia, F.; Venturoli, G.; Melandri, B. A.; Oesterhelt, D. Role of the PufX Protein in Photosynthetic Growth of *Rhodobacter sphaeroides*. 2. PufX is Required for Efficient Ubiquinone/Ubiquinol Exchange Between the Reaction Center Q<sub>B</sub> Site and the Cytochrome *bc*<sub>1</sub> Complex. *Biochemistry* **1995**, *34*, 15248–15258.
- (11) Sauer, K.; Cogdell, R. J.; Prince, S. M.; Freer, A. A.; Isaacs, N. W.; Scheer, H. Structure Based Calculations of the Optical Spectra of the LH2 Bacteriochlorophyll-Protein Complex from *Rhodospseudomonas acidophila*. *Photochem. Photobiol.* **1996**, *64*, 564–576.
- (12) Wu, H.-M.; Ratsep, M.; Lee, I.-J.; Cogdell, R. J.; Small, G. J. Exciton Level Structure and Energy Disorder of the B850 Ring of the LH2 Antenna Complex. *J. Phys. Chem. B* **1997**, *101*, 7654–7663.
- (13) Jang, S.; Silbey, R. J. Single Complex Line Shapes of the B850 Band of LH2. *J. Chem. Phys.* **2003**, *118*, 9324–9336.
- (14) Mostovoy, M. V.; Knoester, J. Statistics of Optical Spectra from Single Ring Aggregates and its Application to LH2. *J. Phys. Chem. B* **2000**, *104*, 12355–12364.
- (15) van Amerongen, H.; Valkunas, L.; van Grondelle, R. *Photosynthetic Excitons*; World Scientific: Singapore, 2000.
- (16) Alden, R. G.; Johnson, E.; Nagarajan, V.; Parson, W. W.; Law, C. J.; Cogdell, R. J. Calculations of Spectroscopic Properties of the LH2 Bacteriochlorophyll-Protein Antenna Complex from *Rhodospseudomonas acidophila*. *J. Phys. Chem. B* **1997**, *101*, 4667–4680.
- (17) Hu, X.; Ritz, T.; Damjanovic, A.; Autenrieth, F.; Schulten, K. Photosynthetic Apparatus of Purple Bacteria. *Q. Rev. Biophys.* **2002**, *35*, 1–62.
- (18) Cogdell, R. J.; Gall, A.; Köhler, J. The Architecture and Function of Purple Bacteria: From Single Molecules to *in vivo* Membranes. *Q. Rev. Biophys.* **2006**, *39*, 227–324.
- (19) Oellerich, S.; Köhler, J. Low-Temperature Single-Molecule Spectroscopy on Photosynthetic Pigment–Protein Complexes from Purple Bacteria. *Photosynth. Res.* **2009**, *101*, 171–179.
- (20) Strümpfer, J.; Şener, M.; Schulten, K. How Quantum Coherence Assists Photosynthetic Light-Harvesting. *J. Phys. Chem. Lett.* **2012**, *3*, 536–542.
- (21) Brotsudarmo, T. H. P.; Kunz, R.; Böhm, P.; Gardiner, A. T.; Moulisová, V.; Cogdell, R. J.; Köhler, J. Single-Molecule Spectroscopy Reveals that Individual Low-Light LH2 Complexes from *Rhodospseudomonas palustris* 2.1.6. Have a Heterogeneous Polypeptide Composition. *Biophys. J.* **2009**, *97*, 1491–1500.
- (22) Richter, M. F.; Baier, J.; Prem, T.; Oellerich, S.; Francia, F.; Venturoli, G.; Oesterhelt, D.; Southall, J.; Cogdell, R. J.; Köhler, J. Symmetry Matters for the Electronic Structure of Core Complexes



from Rhodopseudomonas palustris and Rhodobacter sphaeroides PufX. *Proc. Natl. Acad. Sci. U.S.A.* **2007**, *104*, 6661–6665.

(23) Richter, M. F.; Baier, J.; Southall, J.; Cogdell, R. J.; Oellerich, S.; Köhler, J. Refinement of the X-Ray Structure of the RC-LH1 Core Complex from Rhodopseudomonas palustris by Single-Molecule Spectroscopy. *Proc. Natl. Acad. Sci. U.S.A.* **2007**, *104*, 20280–20284.

(24) Matsushita, M.; Ketelaars, M.; van Oijen, A. M.; Köhler, J.; Aartsma, T. J.; Schmidt, J. Spectroscopy on the B850 Band of Individual Light-Harvesting 2 Complexes of Rhodopseudomonas acidophila: II. Exciton States of an Elliptically Deformed Ring Aggregate. *Biophys. J.* **2001**, *80*, 1604–1614.

(25) Ketelaars, M.; Hofmann, C.; Köhler, J.; Howard, T. D.; Cogdell, R. J.; Schmidt, J.; Aartsma, T. J. Spectroscopy on Individual Light-Harvesting 1 Complexes of Rhodopseudomonas acidophila. *Biophys. J.* **2002**, *83*, 1701–1715.

(26) Jang, S.; Silbey, R. J.; Kunz, R.; Hofmann, C.; Köhler, J. Is There Elliptic Distortion in the Light Harvesting Complex 2 of Purple Bacteria? *J. Phys. Chem. B* **2011**, *115*, 12947–12953.

(27) Dempster, S. E.; Jang, S.; Silbey, R. J. Single Molecule Spectroscopy of Disordered Circular Aggregates: A Perturbation Analysis. *J. Chem. Phys.* **2001**, *114*, 10015–10023.

(28) Bakalis, L. D.; Coca, M.; Knoester, J. Optical Line Shapes of Dynamically Disordered Ring Aggregates. *J. Chem. Phys.* **1999**, *110*, 2208–2218.

(29) Knoester, J.; Agranovich, V. M. *Thin Films and Nanostructures*; Elsevier: Amsterdam, 2003; Vol. 31, pp 1–96.

(30) van Oijen, A. M.; Ketelaars, M.; Köhler, J.; Aartsma, T. J.; Schmidt, J. Unraveling the Electronic Structure of Individual Photosynthetic Pigment-Protein Complexes. *Science* **1999**, *285*, 400–402.

(31) Scherf, U.; Riechel, S.; Lemmer, U.; Mahrt, R. F. Conjugated Polymers: Lasing and Stimulated Emission. *Curr. Opin. Solid State Mater. Sci.* **2001**, *5*, 143–154.

(32) Freiberg, A.; Timpmann, K. Picosecond Fluorescence Spectroscopy of Light-Harvesting Antenna Complexes from Rhodospirillum rubrum in the 300–4 K Temperature Range. Comparison with the Data on Chromatophores. *J. Photochem. Photobiol. B* **1992**, *15*, 151–158.

(33) Vulto, S. I. E.; Kennis, J. T. M.; Streltsov, A. M.; Amesz, J.; Aartsma, T. J. Energy Relaxation Within the B850 Absorption Band of the Isolated Light-Harvesting Complex LH2 from Rhodopseudomonas acidophila at Low Temperature. *J. Phys. Chem. B* **1999**, *103*, 878–883.

(34) Sundström, V.; Pullerits, T.; van Grondelle, R. Photosynthetic Light-Harvesting: Reconciling Dynamics and Structure of Purple Bacterial LH2 Reveals Function of Photosynthetic Unit. *J. Phys. Chem. B* **1999**, *103*, 2327–2346.

(35) Ketelaars, M.; van Oijen, A. M.; Matsushita, M.; Köhler, J.; Schmidt, J.; Aartsma, T. J. Spectroscopy on the B850 Band of Individual Light-Harvesting 2 Complexes of Rhodopseudomonas acidophila: I. Experiments and Monte-Carlo Simulations. *Biophys. J.* **2001**, *80*, 1591–1603.

(36) Blankenship, R. E. *Molecular Mechanisms of Photosynthesis*, Blackwell Science: Oxford, 2002.

(37) Howard, T. D.; McAuley, K.; Cogdell, R. J. *Membrane Transport*; Baldwin, S., Ed.; Oxford University Press: Oxford, 2000; pp 269–307.

(38) Janosi, L.; Kosztin, I.; Damjanovic, A. Theoretical Prediction of Spectral and Optical Properties of Bacteriochlorophylls in Thermally Disordered LH2 Antenna Complexes. *J. Chem. Phys.* **2006**, *125*, 014903–11.

(39) Hofmann, C.; Aartsma, T. J.; Köhler, J. Energetic Disorder and the B850-Exciton States of Individual Light-Harvesting 2 Complexes from Rhodopseudomonas acidophila. *Chem. Phys. Lett.* **2004**, *395*, 373–378.

(40) Richter, M. F.; Baier, J.; Cogdell, R. J.; Köhler, J.; Oellerich, S. Single-Molecule Spectroscopic Characterization of Light-Harvesting 2 Complexes Reconstituted Into Model Membranes. *Biophys. J.* **2007**, *93*, 183–191.

(41) Fotiadis, D.; Qian, P.; Philippsen, A.; Bullough, P. A.; Engel, A.; Hunter, C. N. Structural Analysis of the Reaction Center Light-Harvesting Complex I Photosynthetic Core Complex of Rhodospirillum rubrum Using Atomic Force Microscopy. *J. Biol. Chem.* **2004**, *279*, 2063–2068.